

TG-NAS: Leveraging Zero-Cost Proxies with Transformer and Graph Convolution Networks for Efficient Neural Architecture Search

Ye Qiao[✉], Haocheng Xu[✉], and Sitao Huang[✉]

University of California, Irvine, Irvine CA 92697, USA

Abstract. Neural architecture search (NAS) is an effective method for discovering new convolutional neural network (CNN) architectures. However, existing approaches often require time-consuming training or intensive sampling and evaluations. Zero-shot NAS aims to create training-free proxies for architecture performance prediction. However, existing proxies have suboptimal performance, and are often outperformed by simple metrics such as model parameter counts or the number of floating-point operations. Besides, existing model-based proxies cannot be generalized to new search spaces with unseen new types of operators without golden accuracy truth. A universally optimal proxy remains elusive. We introduce TG-NAS, a novel model-based universal proxy that leverages a transformer-based operator embedding generator and a graph convolution network (GCN) to predict architecture performance. This approach guides neural architecture search across any given search space without the need of retraining. Distinct from other model-based predictor subroutines, TG-NAS itself acts as a zero-cost (ZC) proxy, guiding architecture search with advantages in terms of data independence, cost-effectiveness, and consistency across diverse search spaces. Our experiments showcase its advantages over existing proxies across various NAS benchmarks, suggesting its potential as a foundational element for efficient architecture search. TG-NAS achieves up to $300\times$ improvements in search efficiency compared to previous SOTA ZC proxy methods. Notably, it discovers competitive models with 93.75% CIFAR-10 accuracy on the NAS-Bench-201 space and 74.5% ImageNet top-1 accuracy on the DARTS space.

Keywords: zero-cost proxy · neural architecture search · transformer

1 Introduction

Deep convolutional neural networks (CNN) have achieved incredible performance in computer vision, speech recognition, object detection, and many other fields [12, 16, 25, 34]. Since then many manually designed CNN topologies that target either high performance or high computational efficiency have been proposed [10, 38]. With larger and deeper expert-designed CNN models, people can easily achieve state-of-the-art performance in image classification, object detection, and many other applications. However, manual network architecture design

is costly and requires a significant amount of time, expertise, and computing resources. It becomes even more challenging if the neural network is designed for hardware platforms with stringent resource and energy constraints. Thus neural architecture search (NAS) was proposed to automate the model design and provide an opportunity to explore specialized model architectures within certain performance and resource constraints [23, 41]. Despite the advancements in automated search techniques, the majority of neural architecture search (NAS) approaches still face the challenge of time-consuming training and evaluation. In the early stage, the prevailing methodology involved iteratively sampling DNN architectures from the search space, training them, and using their performance to guide the search process [22]. These approaches were primarily based on reinforcement learning (RL) or evolutionary algorithms.

In recent years, zero-shot proxies [15, 31, 35, 46] have emerged as a promising technique in neural architecture search (NAS). Zero-shot proxies use lightweight computation, typically a single forward pass with one minibatch of data, to assign a score to each DNN architecture in the search space. The scores obtained from these proxies are expected to correlate with the final accuracy of candidate architectures [15, 31, 46]. This approach not only conserves computational resources but also accelerates the overall NAS process, enabling researchers to explore a larger number of architectures. However, recent general zero-shot proxies struggle to consistently perform well for practical uses. Many of them cannot outperform a naïve proxy like the number of parameters (Params) and are often data-dependent and not fast enough. The generally high dependence and correlation of different zero-cost (ZC) proxies from similar domains, such as gradient information or kernel methods [7, 18], may also compromise the effectiveness of zero-shot NAS approaches.

To address these limitations of zero-cost performance indicators, many model-based performance predictors have emerged. These predictors rely on training models to forecast the final validation accuracy of an architecture solely based on its topology and operators. Common models include Gaussian processes [20], deep neural networks [30, 40], among others. However, these methods are not zero-shot and cannot be considered zero-cost since they typically require hundreds of fully-trained architectures as training data, resulting in prolonged search times. Additionally, model-based prediction has often been used only to accelerate NAS query times, given their lack of generalization and inability to handle unseen operators that are not encoded during predictor model training.

This leads us to deep think: how can we develop a pure universal prediction model capable of predicting any given architecture? Is it possible to develop a generally applicable model-based predictor that can handle the aforementioned unseen operator and break the generalization limitations? In other words, why let model-based predictors settle for a subroutine when it has the potential to take the center stage? Our response to these questions is TG-NAS, a model-based predictor-only NAS framework that can be generalized to new search spaces and unseen operators without retraining. It features a general transformer operator encoder and a graph convolution network (GCN) trainer. This novel

approach offers an exceptionally efficient and zero-cost solution to general neural architecture search problems and bridges the gap between model-based predictors and ZC proxies. We will open source this work to facilitate future research. Link to the source code can be found in the supplementary materials.

The main contributions of TG-NAS can be summarized as follows:

- We propose a universally applicable, data-independent performance predictor model that can handle unseen operators in new search spaces without retraining. The model features a graph convolutional network (GCN), an architecture encoder, and a transformer-based operator embedding generator.
- Our proposed model acts as a zero-cost proxy, guiding architecture search. This opens up a new space for prediction model-only architecture search, and we provide a comprehensive analysis on proxy independence.
- We propose a pruning-evolutionary hybrid searching method, enabling quick and accurate identification of the best architecture within the search space.
- Our analysis of TG-NAS proxies demonstrates remarkable performance on both NAS-Bench-201 and DARTS spaces with CIFAR-10/ImageNet datasets. TG-NAS achieves up to $300\times$ faster search compared to other zero-cost proxies and up to $331,200\times$ faster than other NAS methods, while maintaining high accuracy.

2 Background and Related Work

2.1 Neural Architecture Search (NAS)

Conventional NAS algorithms are an important step in automating the design of neural architectures for a given task [46]. A typical NAS contains a **search strategy** that selects the candidate neural architecture from a predefined **search space** and an **estimation strategy** that enables the performance estimation for the current candidate.

Search space can be categorized as the following types: macro search space [13], chain-structures search space [38], cell-based search space [8, 28, 53], and hierarchical search space [27]. Among those, cell-based search space is the most popular one in NAS [46]. The searchable cells (a directed acyclic graph of operations) make up the microstructure of the search space while the macrostructure (ways and number of cells to stack together) is fixed. For example, NAS-Bench-101 [53] contains 423,624 unique architectures, and each cell consists of 7 nodes (each node chosen from 3 operators). In NAS-Bench-201 [8], there are 15,625 cell candidates and each cell consists of 4 nodes (each node chosen from 5 operators). In contrast, the DARTS search space [28] is more expansive, featuring approximately 10^{18} architectures. It consists of two cells, each containing seven nodes. The first two nodes receive inputs from previous layers, and the intermediate four nodes can assume any DAG structure, each having two incident edges. The last node serves as the output node, and each edge can take on one of eight operations. In this work, we perform our experiments on those three search spaces for different purposes.

The **search strategy** in NAS has been widely explored. There are some well-known black-box optimizations, such as random selection with full training, reinforcement learning, evolution, Bayesian optimization, and Monte Carlo tree search. With these search strategies, we still need to train the searched architecture and use the performance result to guide the search, which is a time-consuming process. To overcome the training time bottleneck, one-shot techniques were introduced as an **estimation strategy**. These techniques involve training a single (one-shot) supernet, which is an over-parameterized architecture that encompasses all possible architectures in the search space [2, 3, 28]. Once the supernet has been trained, each architecture in the search space can be evaluated by inheriting its weights from sampling the subnet within the supernet.

2.2 Zero-Cost (ZC) Proxies for NAS

However, the training of the supernet still takes up the majority of the NAS runtime. To speed up the entire NAS process, a more efficient **estimation strategy** to predict the performance of the searched architecture is needed. Recently, zero-cost proxies have been introduced as a family of performance prediction techniques. The idea is to avoid training any neural network and to run a fast computation (one single forward pass over certain data) over the searched architecture that can assign a ranking or score to each searched architecture.

The expressivity of a neural network, which relates to the complexity of the function it can represent, has been widely used as one of the zero-cost proxies. Several recent works, such as TE-NAS [4], ZEN-NAS [24], and NASWOT [31], approximate the behavior of neural networks by considering the expressivity of ReLU network and the number of linear regions they can separate. Kernel methods have also been employed to approximate the convergence and generalization ability of networks without training. For instance, TE-NAS [4], formulates neural networks as a Gaussian process [17, 52] and analyzes randomly-initialized architectures by the spectrum of the neural tangent kernel (NTK) [11, 48] and the number of linear regions in the input space. Zico [21] extends such kernel-based analysis to reveal the relationships between the gradient properties and the training convergence and generalization capacity of neural networks. Similarly, gradient with respect to the parameters of neural networks is proved to be different approximations of Taylor expansion of deep neural networks [1, 18, 44]. SNIP [18] introduced a saliency metric computed at initialization using a single minibatch of data; Grasp [44] improved upon SNIP [18] by approximating the change in gradient norm instead of loss; Synflow [1] generalized previous approaches and proposed a modified version computes a loss which is simply the product of all parameters in the network thus no data is needed. Gradient concerning feature maps combined with the number of linear regions have been used in Zen-NAS [24]. There are also other zero-cost proxies considering Jacobian covariances, fisher information, and other important theoretical indicators [1, 31, 42]. Although zero-cost proxies can expedite estimation time, they often compromise prediction accuracy and introduce biases stemming from data dependency [46].

2.3 Issue of Model-based Prediction and Unseen Operators

Despite the inherent limitations of zero-cost performance prediction, the integration of model-based prediction has emerged as a pivotal component in guiding neural architecture search (NAS) algorithms. This approach is particularly useful when combined with Bayesian optimization and utilized as a subroutine [13, 40]. Various types of predictor models, including Gaussian processes (GP), multi-layer perceptron (MLP), long short-term memory (LSTM) networks, and graph neural networks (GNN), have been employed. Typically, as the algorithm progresses and a set of fully evaluated architectures becomes available, a meta-model is trained using architecture topology as features and validation accuracies as labels. This model is then used to predict the validation accuracy of yet-to-be-evaluated architectures. Notably, White et al. [47] demonstrated that augmenting the model with Jacobian covariance as an additional feature can enhance its performance by up to 20%. Shen et al. [39] further extended this approach by integrating zero-cost proxies into Bayesian optimization, resulting in $3\text{-}5\times$ speedups over previous methods.

Existing model-based predictor approaches exhibit notable biases, limiting their effectiveness to specific search spaces and requiring fully evaluated architectures as labels. The high initialization time is also a concern. Dudziak et al. [9] attempted to address this issue by leveraging the model’s binary relation and training a prediction model through iterative data selection. However, their approach still requires over 6 GPU days to conduct the search process. Furthermore, due to simplistic architecture and feature embedding methods, such as one-hot encoding, these models cannot process unseen operators. These limitations prompt us to explore a more robust operator encoding method that enables a pretrained prediction model to operate effectively in any architecture search space and accommodate unseen operators. Essentially, we investigate the viability of relying solely on pretrained model-based prediction as a universal zero-cost proxy for guiding searches across diverse architecture spaces with negligible search time.

3 TG-NAS: A General Zero-Cost Proxy

In this work, we propose TG-NAS, a general zero-cost proxy method for neural architecture search with a transformer embedding generator and a graph neural network trainer, supporting unseen operators in new search spaces. The embedding generator produces the desired feature embeddings with various techniques and the GCN trainer functions as a model-based predictor to predict the accuracy (or ranking) of a given architecture. Finally, the data-independent predicted ranking will guide the search algorithm as shown in Fig. 8.

3.1 Architecture Representation

Various neural architecture search work represent their networks in the cell structure. For instance, DARTS [28], and NATS-Bench (NAS-Bench-201) [6, 8] define a cell-based search space representing each architecture as a directed acyclic

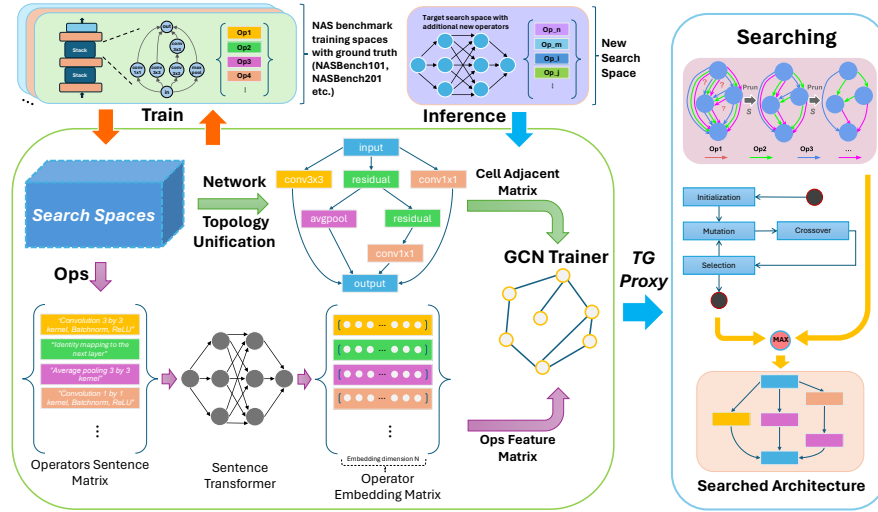


Fig. 1: TG-NAS Framework

graph (DAG), with nodes representing the features. NAS-Bench-101 [53] on the other hand utilizes nodes to represent layers (operators) and edges for forward dataflow propagation. BANANAS [45] proposed a novel path-based encoding scheme and claimed it scales better than other methods.

In this work, we represent the DNN architecture candidates using DAG with nodes representing operators and edges corresponding to model data propagation flow. We then represent the graphs with adjacent matrix and operator node embeddings, which becomes data input for our graph convolution network (GCN) [14] trainer. To make all search space comply with this representation, TG-NAS unifies other cell-based search space representations as shown in Fig. 8. We applied this transformation to both NAS-Bench-201 and DARTS space in this work. NAS-Bench-101 was provided with the aforementioned architecture graphs, therefore no transformation is needed. Fig. 8 shows an example on NAS-Bench-201. The final model architectures of each search space are obtained by stacking multiple repeated cells with some other predefined cells in between. The differences between different DNN architecture candidates are purely determined by the cell architecture (represented as graph), so we use the embedding of individual cell architectures (as graphs) to represent the entire DNN architecture. Operator node features are encoded using a transformer model with a fixed length embedding size. The details can be seen in the following section.

3.2 Operator Embedding Generator

In our approach, we encode model cell graphs using an adjacency matrix together with node embeddings. However, encoding operators demand special attention

as it involves representing and distinguishing various deep learning operators. Previous methods, which typically rely on one-hot vectors for operator encoding, are deemed suboptimal and non-portable, especially when dealing with unseen search spaces and operators.

Recognizing that the names of operators inherently contain valuable information, we assert that the **operator name** alone can provide insight into the operation. For instance, the operator name “*CONV3x3-BN-ReLU*” suggests that it contains a two-dimensional convolution with a 3x3 kernel, followed by batch normalization and rectified linear activation. Therefore, we propose to construct a robust embedding model capable of extracting internal semantic information from operator names or their descriptive sentences in natural languages. For example, in the high-dimensional encoding space, operators like *conv3x3* are expected to be closer to *conv5x5* than to *maxpool3x3*. Additionally, if the embedding model comprehends one type of operator, it should readily extend its knowledge to similar operators with, for example, different kernel sizes.

Table 1: Operator Descriptive Sentences Vary in Length for Generating Embedding

| Operators | Short Sentences | Medium Sentences | Long Sentences |
|--------------|-----------------------|--|--|
| none | "None" | "Doing nothing" | "A none operator that does nothing" |
| skip_connect | "Residual connection" | "Identity mapping to the next layer" | "A residual connection operator that adds identity mapping to the next layer" |
| nor_conv_3x3 | "Convolution 3x3" | "Convolution 3 by 3 kernel, Batchnorm, ReLU" | "A two-dimensional convolutional operator with a kernel size of 3 by 3 is applied, succeeded by a batch normalization layer, and followed by a rectified linear layer" |
| nor_conv_1x1 | "Convolution 1x1" | "Convolution 1 by 1 kernel, Batchnorm, ReLU" | "A two-dimensional convolutional operator with a kernel size of 1 by 1 is applied, succeeded by a batch normalization layer, and followed by a rectified linear layer" |
| avg_pool_3x3 | "Average pooling 3x3" | "Average pooling 3 by 3 kernel" | "A average pooling operator with a kernel size 3 by 3" |

Table 2: Results of Different Combination of Sentences Transformer Model and Embedding Sentence Length

| Sentence Transformer Model | Model Size (MB) | Embedding Size | Kendall’s τ | | | Spearman’s ρ | | |
|----------------------------|-----------------|----------------|------------------|--------|------|-------------------|--------|------|
| | | | Short | Medium | Long | Short | Medium | Long |
| all-mpnet-base-v2 | 420 | 768 | 0.48 | 0.49 | 0.46 | 0.66 | 0.67 | 0.65 |
| MiniLM-L6-v2 | 80 | 384 | 0.57 | 0.44 | 0.40 | 0.77 | 0.62 | 0.56 |
| MiniLM-L6-v2-64 | 81 | 64 | 0.36 | 0.29 | 0.32 | 0.54 | 0.43 | 0.47 |

Certain existing works have attempted to construct embedding vectors from words or sentences, such as GloVe [33], or employed character embeddings to capture fine-grained semantic and syntactic regularities. However, our earlier experiments indicated that these methods face challenges when dealing with unseen words, particularly operators in our case. Consequently, we have opted for Sentence BERT [37] as our primary method for generating desired operator embeddings. As illustrated in Fig. 8, the Sentence Transformer utilizes siamese and triplet network structures to derive semantically meaningful sentence embeddings that can be compared using cosine similarity. A pooling operation is applied to the output of the pretrained transformer model to obtain a fixed-sized sentence embedding. We compute the mean of all output word vectors as the pooling strategy to generate the final operator embedding.

In our experiments, we explore three different sizes of pretrained sentence transformer models and three distinct operator sentence lengths, crucial for

embedding generation analysis. As outlined in Table 1, we define and experiment with short, medium, and long operator descriptions as inputs to the embedding generator model. The test results on NAS-Bench-201 are presented in Table 2. All three models undergo pretraining on the same 25 dataset collections [37], containing over 1 billion training sentence pairs in total. The triplet objective function is employed during the pretraining phase. This function, given an anchor sentence a , a positive sentence p , and a negative sentence n , tunes the network to ensure that the distance between a and p is smaller than the distance between a and n . Mathematically, the loss function can be expressed as:

$$\mathcal{L} = \max(\|s_a - s_p\| - \|s_a - s_n\| + \epsilon) \quad (1)$$

where s_i 's are the sentence embeddings for a , n , and p respectively, and $\|\cdot\|$ denotes a distance metric and ϵ represents a margin. The chosen margin ϵ ensures that s_p is at least ϵ closer to s_a than s_n . In this context, the Euclidean distance serves as the distance metric, and ϵ is specifically set to 1 during training.

The *all-MiniLM-L6-v2-64* entries in Table 2 are downsampled from the original *all-MiniLM-L6-v2* model using principal component analysis (PCA) to achieve a 64-dimensional embedding vector length. The results of our GCN model prediction ranking (which we will discuss in the next section), trained with NAS-Bench-101 and tested on NAS-Bench-201, are presented in Table 2. Notably, the combination of short sentence embedding and the pretrained *all-MiniLM-L6-v2-64* sentence transformer model, with embedding length of 384, yields the best results for both Kendall's τ and Spearman's ρ correlation coefficients. Our later experiments will adopt this combination.

Furthermore, we anticipate that fine-tuning the embedding model with context containing specific knowledge about deep learning operators would further enhance the performance of our proposed approach. We leave this area as a potential direction for future research.

3.3 GCN Proxy Trainer

After completing the universal architecture encoding and operator feature embedding, we employ a two-layer graph convolution network (GCN) as our prediction model. With normalization trick, GCN can be defined as

$$H = X *_G G_\theta = f(\bar{A}X\theta), \quad (2)$$

where $\bar{A} = \tilde{D}^{-\frac{1}{2}} \tilde{A} \tilde{D}^{-\frac{1}{2}}$, $\tilde{A} = A + I_n$, and $\tilde{D}_{ii} = \sum_j \tilde{A}_{ij}$. To prevent overfitting to a particular training space, we incorporate graph normalization [5] and weight decay techniques. Our overarching objective is to deliver a universally applicable pretrained predictor model that requires no tuning for new search spaces. Consequently, the GCN predictor model is subject to heavy regularization. An additional crucial factor influencing our choice of GCN over other prediction models is its capability to handle vast differences in architectures. Given the varying dimensions of the adjacency matrix (from unseen search spaces) and operator matrix (from unseen operators), GCN emerges as a suitable choice, demonstrating flexibility in accommodating diverse architectural structures.

To assess the predictor’s applicability, we partition the NAS-Bench-101 space into train/validation splits ranging from 90% to 1%. The results, depicted in Fig. 2, demonstrate the predictor’s effectiveness, even when trained on only 1% of the architecture data. This is evident in the strong performance indicated by Kendall’s τ and Spearman’s ρ correlation coefficients. Exploring the use of different graph neural networks (GNNs) such as graph attention network (GAT) [43] may yield different results and behaviors. We consider this as an open area for further investigation.

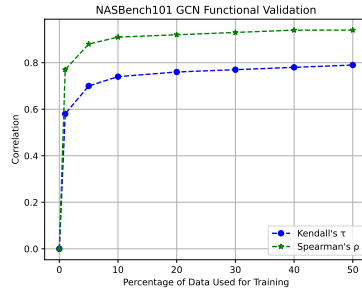


Fig. 2: GCN Predictor Functional Validation on NAS-Bench-101

3.4 Pruning-Evolutionary Hybrid Searching

The search strategy generally falls into two types. The first type involves applying black-box optimization techniques (reinforcement learning and evolution search etc.) in conjunction with a sampling-based method to explore the predefined search space. These methods sample and evaluate architectures to optimize the searching agent’s reward. The other type is close to one-shot techniques, where a hypernetwork will be introduced with architecture representation relaxation to enable searching using gradient descent. It can be applied to all DAG-based search spaces [28] due to its continuous hyperparameter for the architecture. However, when considering the cell-based search space, the computational burden of these sampling-based one-shot methods remains dependent on the scale of the search space and hence it has limited effectiveness. Consider a network comprising interconnected cells in a directed acyclic graph structure. Each cell contains E edges, with each edge selecting a single operator from a set of $|O|$ potential candidates. Consequently, there are $|O|^E$ distinct cells, and during the sampling-based search process, $\alpha|O|^E$ networks must be sampled. The parameter α represents the sampling process efficiency, where a smaller value can help find superior architectures faster.

Meanwhile, evolutionary and genetic algorithms have been commonly used to optimize the NAS [46]. To enhance the efficiency of the search, we propose a pruning-evolutionary hybrid searching method. The pruning method, inspired by [19], reduces the search cost from $\alpha|O|^E$ to $|O| \cdot E$. Algorithm 1 shows our proposed algorithm.

For the pruning search part, we start with a supernet N_{init} encompassing all possible operators for each edge. Then we iteratively prune one operator on each edge until the current supernet N_t transforms into a single-path network, representing the final searched architecture. For the evolutionary search part, we first **initialize** the entire population of architecture candidates with continuous parameters, where we map all operators evenly into the value between 0 and 1. Then **mutation** operation and **crossover** operation are performed to produce a new child. After generating all the offspring, the selection process will kick in

using our proposed proxy to select the elite candidates for the next generation. After finishing both parts of searching, we select the final architecture from the best of the two search results. This hybrid searching method is valid and efficient due to the effectiveness of the proposed zero-cost proxy.

Algorithm 1: TG-NAS Pruning-Evolutionary Hybrid Search Algorithm

Data: M_0 supernet, E edges in each cell, every edge have O operators
while M_t is not a single path network **do**
 for $Cell_type, ct$ **in** M_t **do**
 for edge E_i , operator O_j **in** ct, E_i **do**
 for operator O_j **in** E_i **do**
 $P_{t,e_i,o_j} \leftarrow GCN_Inference(M_{t,e_i,o_j});$
 $\Delta P_{t,e_i,o_j} \leftarrow P_{t,e_i,o_j} - P_{t,e_i \setminus o_j};$
 end for
 end for
 Rank \leftarrow index of o_j in descending of ΔP_t ;
 end for
 for e_i **in** E **do**
 $o_p \leftarrow argmin\{S(o_p) \mid o_p \in e_i\};$
 $M_{t+1} \leftarrow M_t - o_p$;
 end for
 $t \leftarrow t + 1$;
end while
Data: NP population size
 $g \leftarrow 0$;
while $|pop| < NP$ **do**
 $pop_i \leftarrow random_configuration();$
 $pop'_i \leftarrow discretized_architecture(pop_i);$
 $fitness_i \leftarrow GCN_Inference(pop'_i);$
end while
while $g < g_{max}$ **do**
 $V_g \leftarrow mutate(pop_g);$
 $U_g \leftarrow crossover(V_g, pop_g);$
 $U'_g \leftarrow discretized_population(U_g);$
 $fitness_g \leftarrow GCN_Inference(U'_g);$
 $pop_{g+1}, fitness_{g+1} \leftarrow select(pop_g, U_g);$
end while
return $Max(M_t, POP_g);$

4 Experiment and Results Analysis

4.1 Independent Analysis and Combination with other proxies

Multiple proxies could be combined to enhance the performance prediction accuracy. However, certain proxies could be highly correlated and do not provide

extra information. Therefore, not all combinations provide good performance. We conducted assessments of zero-cost proxies on NAS-Bench-201 search spaces using the aforementioned three datasets. Additionally, by evaluating the same search space across different tasks, we aimed to determine if data- and task-independent zero-cost proxies offer universally applicable rankings. Our evaluation encompassed 14 zero-cost proxies, including our TG-NAS proxy result. We randomly sampled 1000 architectures from the search space and evaluated each zero-cost proxy metric for each architecture. Subsequently, we computed the *Spearman's* rank correlation between each proxy.

Our analysis revealed a trend where the rank correlations of some zero-cost proxies were highly correlated, such as *flops* (number of floating-point operations) and *params* (model parameter count), which is expected due to the relationship between parameters and computation in deep learning. This prompted us to compute the full correlations between all 14 pairs of zero-cost proxies and analyze their behaviors.

Fig. 10 shows the heatmap of correlations between pairs of popular proxies (calculated with CIFAR-10 results; CIFAR-100 and ImageNet16-120 results are available in the supplementary materials). We observed a consistent trend where *flops* and *params* exhibited high correlations with each other. Additionally, *synflow* [1] often showed high correlations with *flops* and *params*, consistent with recent work by Ning et al. [32], which demonstrated that *synflow's* value increases with the number of parameters in the architecture. We also noted high correlations between *grad_norm* [1], *snip* [18], *grasp* [44], *nwot* [31], and *fisher* [42], occasionally with *l2_norm* [1] as well, as they all leverage gradient saliency matrix information. Moreover, *epe_nas* [29] and jacobian covariance (*jacov*) [31] were highly correlated with each other.

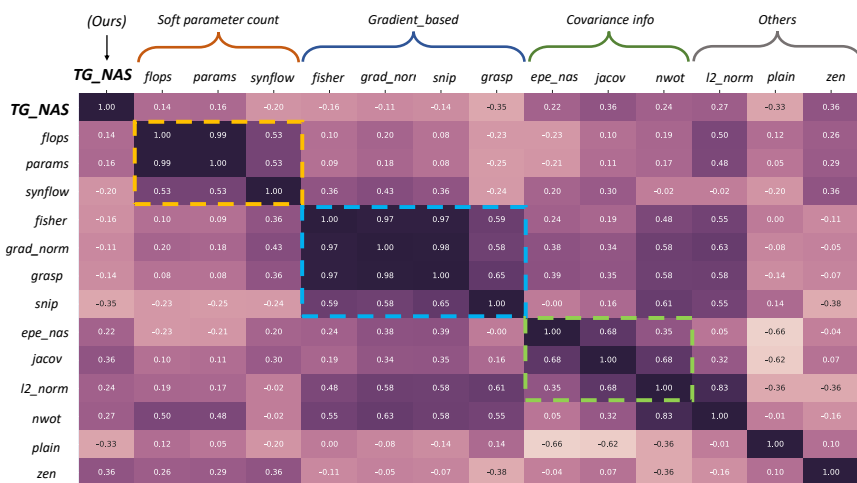


Fig. 3: Spearman's ρ Correlation for All Pairs of ZC Proxies on NAS-Bench-201

It’s intriguing to note that the *zen* score [24] and our TG-NAS proxy demonstrated the highest level of independence among all proxies evaluated. This suggests that our method offers a unique perspective on understanding model architectures. This discovery holds the potential to provide new insights into the design of zero-cost neural architecture search and the analysis of optimal combinations of zero-cost proxies. This could lead to further enhancements in zero-shot NAS techniques overall. We haven’t included some zero-cost proxies due to various reasons: they either require training of supernet to make an evaluation or they did not release the source code [3, 9, 40, 51].

Table 3: Kendall’s τ and Spearman’s ρ correlation between various zero-cost proxies

| Proxy Name | Params | FLOPs | SNIP | Fisher | Synflow | Zen-score | grad-norm | TG-NAS (ours) |
|-------------------|--------|-------|------|--------|---------|-----------|-----------|---------------|
| Kendall’s τ | 0.55 | 0.54 | 0.41 | 0.22 | 0.54 | 0.29 | 0.37 | 0.57 |
| Spearman’s ρ | 0.74 | 0.73 | 0.58 | 0.36 | 0.73 | 0.38 | 0.54 | 0.77 |

4.2 Result Analysis of CIFAR-10 on NAS-Bench-201 Space

For testing on NAS-Bench-201, our predictor model was trained using the entire NAS-Bench-101 architecture set, and the obtained predictions were employed to guide the search on the new space, NAS-Bench-201, using the proposed method. The Kendall’s τ and Spearman’s ρ correlation scores displayed in Table 3 indicate that our TG proxy outperforms other zero-cost proxies when evaluated on NAS-Bench-201 spaces. Fig. 4 demonstrates that our TG proxy is highly positively correlated with the architecture’s test accuracy. Additionally, as illustrated in Table 4, our TG-NAS outperforms the majority of zero-shot NAS approaches and is comparable to the state-of-the-art TE-NAS results, achieving 93.75% top-1 accuracy on CIFAR-10, while consuming only a fraction of the searching time of prior works.

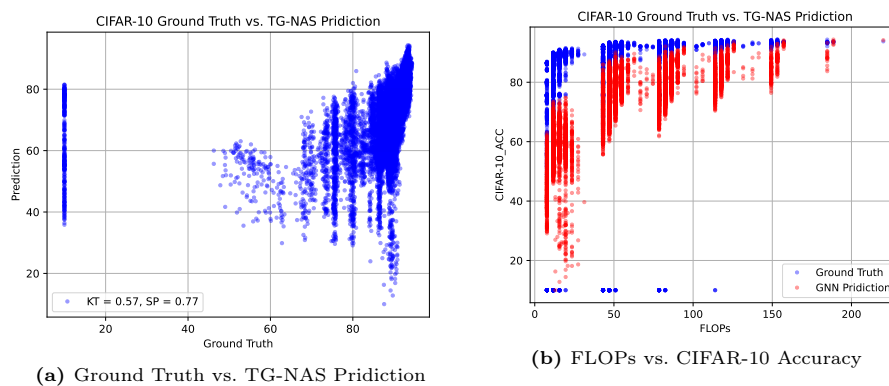


Fig. 4: TG-NAS Correlation Evaluation with Ground Truth on NAS-Bench-201 Space

Notably, despite the efficiency claims of zero-cost NAS methods over conventional NAS due to avoiding the training of sampled architectures, variations in computational cost and search time persist among them. For example, TE-NAS [4] required over 4 GPU hours, while ZiCo [21] demanded over 10 GPU hours for the search on ImageNet on the DARTS space. This discrepancy arises from the fact that several proxy computations necessitate at least one forward pass or a forward-backward pass, requiring multiple runs for result stabilization. Additionally, many are data-dependent, limiting their general applicability and extending search times.

In contrast, TG-NAS completed the search in about 40 seconds, achieving up to a 300× speedup compared to other zero-cost methods due to the lightweight nature of the proposed predictor model. Notably, the comparison of search times does not factor in the predictor model training time (the model training required 1.5 GPU hours), as it is a one-time training effort, and the pretrained model can be distributed for uses in various scenarios and search spaces.

Table 4: Results of CIFAR-10, CIFAR-100 and ImageNet16-120 on NAS-Bench-201

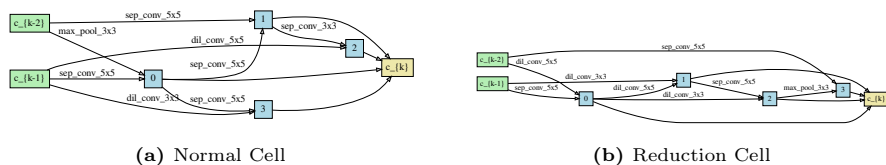
| Name of Works | FLOPs (M) | Params (M) | Search Cost (GPU Hours) | CIFAR-10 Accuracy (%) | CIFAR-100 Accuracy (%) | ImageNet16-120 Accuracy (%) |
|----------------|---------------|--------------|-------------------------|-----------------------|------------------------|-----------------------------|
| μ NAS [22] | 7.78 | 0.073 | 552 | 86.49 | 58.30 | 27.80 |
| DARTS [28] | 82.49 | 0.587 | 3.02 | 88.32 | 67.78 | 34.60 |
| GDAS [7] | 117.88 | 0.83 | 8.03 | 93.36 | 69.64 | 38.87 |
| KNAS [50] | 153.27 | 1.073 | 2.44 | 93.43 | 71.05 | 45.05 |
| NASWOT [31] | 86.43 | 0.615 | 0.09 | 92.96 | 69.70 | 44.47 |
| TE-NAS [4] | 188.66 | 1.317 | 0.43 | 93.78 | 70.44 | 41.40 |
| TG-NAS (ours) | 113.95 | 0.802 | 0.01 | 93.75 | 70.64 | 44.97 |
| Ground Truth | 153.27 | 1.073 | - | 94.37 | 73.22 | 46.71 |

4.3 Result Analysis of ImageNet on DARTS Space

For the DARTS search space, our GCN prediction model undergoes a slightly different training process, incorporating additional data from NAS-Bench-201 into the training set. Consequently, our training dataset comprises a total of 423,000 NAS-Bench-101 architectures and an additional 15,625 architectures from NAS-Bench-201. The labels for the NAS-Bench-101 portion are derived from the CIFAR-10 evaluation accuracy. However, the NAS-Bench-201 labels differ slightly due to additional CIFAR-100 and ImageNet-16-120 results. To mitigate bias arising from the monolithic dataset, we amalgamate the normalized accuracies of CIFAR-10, CIFAR-100, and ImageNet-16-120 to construct a unified ground truth label for NAS-Bench-201 architectures. Indeed, while introducing an additional proxy is necessary due to the absence of actual results on the ImageNet dataset in those NAS benchmarks, it’s worth noting that CIFAR-10/100 performance often serves as a reliable indicator for ImageNet performance. The final discovered cell architecture can be seen in Fig. 5. After the target cell was determined, the final network was constructing by stacking 14 cells, with the initial channel number

Table 5: Comparison with Recent NAS Works on ImageNet with the mobile setting.

| Name of Works | Test Accuracy (%) | | Search Cost (GPU Days) | Params (M) | Search Method |
|------------------|-------------------|-------------|---------------------------|---------------|------------------------------|
| | Top-1 | Top-5 | | | |
| PNAS [26] | 74.2 | 91.9 | 225 | 5.1 | Bayesian Optimization |
| AmoebaNet-C [36] | 75.7 | 92.4 | 3150 | 6.4 | Evolution |
| NASNet-A [55] | 74.0 | 91.6 | 2000+ | 5.3 | Reinforcement Learning |
| DARTS [28] | 73.3 | 91.3 | 4.0 | 4.7 | Gradient-based |
| SNAS [49] | 72.7 | 91.8 | 1.5 | 4.3 | Gradient-based |
| BayesNAS [54] | 73.5 | 91.1 | 0.2 | 3.9 | Gradient-based |
| ProxylessNAS [3] | 75.1 | 92.5 | 8.3 | 7.1 | Gradient-based |
| TE-NAS [7] | 74.2 | 92.2 | 0.17 | 5.4 | Theoretical analysis |
| BONAS-B [40] | 75.2 | 92.7 | 5.0 | 4.5 | Bayesian Optimization |
| PC-DARTS [51] | 74.9 | 92.2 | 0.1 | 5.3 | Gradient-based |
| TG-NAS (ours) | 74.5 | 91.9 | 0.0014 | 5.6 | Model-based Predictor |

**Fig. 5:** Discovered DNN Cell Architecture on the DARTS Space

set to 48. Performance results are shown in Table 5. Our approach achieves a top-1/5 accuracy of 74.5% and 91.9% respectively, comparable to other works on ImageNet. Notably, TG-NAS only took less than 2 minutes of search time on one NVIDIA RTX 4090 GPU. We expect that performance can be further enhanced if incorporating additional training samples from supplementary NAS benchmarks.

5 Conclusion

In this work, We present TG-NAS, a model-based predictor framework that is generally applicable for new search spaces with unseen new operators. It integrates a transformer-based operator embedding generator with a graph convolution network and functions as a ZC proxy. TG-NAS offers advantages in terms of data independence, cost-effectiveness, and generality. Our experiments demonstrate its superiority over existing proxies across various NAS benchmarks, positioning it as a foundational element for efficient architecture search. TG-NAS achieves up to a $300\times$ improvement in search efficiency compared to previous state-of-the-art zero-cost proxy methods. Notably, it discovers competitive models with 93.75% CIFAR-10 accuracy on the NAS-Bench-201 space and 74.5% ImageNet top-1 accuracy on the DARTS space.

References

1. Abdelfattah, M.S., Mehrotra, A., Łukasz Dudziak, Lane, N.D.: Zero-cost proxies for lightweight nas (2021)
2. Cai, H., Gan, C., Wang, T., Zhang, Z., Han, S.: Once-for-all: Train one network and specialize it for efficient deployment (2020)
3. Cai, H., Zhu, L., Han, S.: Proxylessnas: Direct neural architecture search on target task and hardware (2019)
4. Chen, W., Gong, X., Wang, Z.: Neural architecture search on ImageNet in four GPU hours: A theoretically inspired perspective. arXiv preprint arXiv:2102.11535 (2021)
5. Chen, Y., Tang, X., Qi, X., Li, C.G., Xiao, R.: Learning graph normalization for graph neural networks (2020)
6. Dong, X., Liu, L., Musial, K., Gabrys, B.: Nats-bench: Benchmarking nas algorithms for architecture topology and size. *IEEE Transactions on Pattern Analysis and Machine Intelligence* p. 1–1 (2021). <https://doi.org/10.1109/tpami.2021.3054824>, <http://dx.doi.org/10.1109/TPAMI.2021.3054824>
7. Dong, X., Yang, Y.: Searching for a robust neural architecture in four gpu hours. In: *Proceedings of the IEEE/CVF Conference on Computer Vision and Pattern Recognition*. pp. 1761–1770 (2019)
8. Dong, X., Yang, Y.: Nas-bench-201: Extending the scope of reproducible neural architecture search. In: *International Conference on Learning Representations (ICLR)* (2020)
9. Łukasz Dudziak, Chau, T., Abdelfattah, M.S., Lee, R., Kim, H., Lane, N.D.: Brp-nas: Prediction-based nas using gcns (2021)
10. He, K., Zhang, X., Ren, S., Sun, J.: Deep residual learning for image recognition. In: *Proceedings of the IEEE conference on computer vision and pattern recognition*. pp. 770–778 (2016)
11. Jacot, A., Gabriel, F., Hongler, C.: Neural tangent kernel: Convergence and generalization in neural networks (2020)
12. Kaeley, H., Qiao, Y., Bagherzadeh, N.: Support for stock trend prediction using transformers and sentiment analysis. arXiv preprint arXiv:2305.14368 (2023)
13. Kandasamy, K., Neiswanger, W., Schneider, J., Póczos, B., Xing, E.: Neural architecture search with bayesian optimisation and optimal transport (2019)
14. Kipf, T.N., Welling, M.: Semi-supervised classification with graph convolutional networks (2017)
15. Krishnakumar, A., White, C., Zela, A., Tu, R., Safari, M., Hutter, F.: Nas-bench-suite-zero: Accelerating research on zero cost proxies (2022)
16. Krizhevsky, A., Sutskever, I., Hinton, G.E.: Imagenet classification with deep convolutional neural networks. *Advances in neural information processing systems* **25** (2012)
17. Lee, J., Xiao, L., Schoenholz, S., Bahri, Y., Novak, R., Sohl-Dickstein, J., Pennington, J.: Wide neural networks of any depth evolve as linear models under gradient descent. *Advances in neural information processing systems* **32** (2019)
18. Lee, N., Ajanthan, T., Torr, P.H.S.: Snip: Single-shot network pruning based on connection sensitivity (2019)
19. Lee, N., Ajanthan, T., Torr, P.H.: Snip: Single-shot network pruning based on connection sensitivity. In: *ICLR* (2019)
20. Lévesque, J.C., Durand, A., Gagné, C., Sabourin, R.: Bayesian optimization for conditional hyperparameter spaces. In: *2017 International Joint Conference on Neural Networks (IJCNN)*. pp. 286–293. IEEE (2017)

21. Li, G., Yang, Y., Bhardwaj, K., Marculescu, R.: Zico: Zero-shot nas via inverse coefficient of variation on gradients (2023)
22. Liberis, E., Dudziak, L., Lane, N.D.: μ NAS: Constrained Neural Architecture Search for Microcontrollers. In: Proceedings of the 1st Workshop on Machine Learning and Systems. EuroMLSys '21 (2021). <https://doi.org/10.1145/3437984.3458836>
23. Lin, J., Chen, W.M., Cohn, J., Gan, C., Han, S.: MCUNet: Tiny deep learning on iot devices. In: Annual Conference on Neural Information Processing Systems (NeurIPS) (2020)
24. Lin, M., Wang, P., Sun, Z., Chen, H., Sun, X., Qian, Q., Li, H., Jin, R.: Zen-nas: A zero-shot nas for high-performance deep image recognition (2021)
25. Lin, T.Y., Maire, M., Belongie, S., Bourdev, L., Girshick, R., Hays, J., Perona, P., Ramanan, D., Zitnick, C.L., Dollár, P.: Microsoft coco: Common objects in context (2015)
26. Liu, C., Zoph, B., Neumann, M., Shlens, J., Hua, W., Li, L.J., Fei-Fei, L., Yuille, A., Huang, J., Murphy, K.: Progressive neural architecture search. In: Proceedings of the European conference on computer vision (ECCV). pp. 19–34 (2018)
27. Liu, H., Simonyan, K., Vinyals, O., Fernando, C., Kavukcuoglu, K.: Hierarchical representations for efficient architecture search (2018)
28. Liu, H., Simonyan, K., Yang, Y.: Darts: Differentiable architecture search. arXiv preprint arXiv:1806.09055 (2018)
29. Lopes, V., Alirezazadeh, S., Alexandre, L.A.: EPE-NAS: Efficient Performance Estimation Without Training for Neural Architecture Search, p. 552–563. Springer International Publishing (2021). https://doi.org/10.1007/978-3-030-86383-8_44, http://dx.doi.org/10.1007/978-3-030-86383-8_44
30. Ma, L., Cui, J., Yang, B.: Deep neural architecture search with deep graph bayesian optimization. In: IEEE/WIC/ACM International Conference on Web Intelligence. pp. 500–507 (2019)
31. Mellor, J., Turner, J., Storkey, A., Crowley, E.J.: Neural architecture search without training (2021)
32. Ning, X., Tang, C., Li, W., Zhou, Z., Liang, S., Yang, H., Wang, Y.: Evaluating efficient performance estimators of neural architectures (2021)
33. Pennington, J., Socher, R., Manning, C.D.: Glove: Global vectors for word representation. In: Proceedings of the 2014 conference on empirical methods in natural language processing (EMNLP). pp. 1532–1543 (2014)
34. Qiao, Y., Alnemari, M., Bagherzadeh, N.: A two-stage efficient 3-d cnn framework for eeg based emotion recognition. In: 2022 IEEE International Conference on Industrial Technology (ICIT). IEEE (2022)
35. Qiao, Y., Xu, H., Zhang, Y., Huang, S.: Micronas: Zero-shot neural architecture search for mcus (2024)
36. Real, E., Aggarwal, A., Huang, Y., Le, Q.V.: Regularized evolution for image classifier architecture search. In: Proceedings of the aaai conference on artificial intelligence. vol. 33, pp. 4780–4789 (2019)
37. Reimers, N., Gurevych, I.: Sentence-bert: Sentence embeddings using siamese bert-networks (2019)
38. Sandler, M., Howard, A., Zhu, M., Zhmoginov, A., Chen, L.C.: Mobilenetv2: Inverted residuals and linear bottlenecks (2019)
39. Shen, Y., Li, Y., Zheng, J., Zhang, W., Yao, P., Li, J., Yang, S., Liu, J., Cui, B.: Proxybo: Accelerating neural architecture search via bayesian optimization with zero-cost proxies (2023)

40. Shi, H., Pi, R., Xu, H., Li, Z., Kwok, J., Zhang, T.: Bridging the gap between sample-based and one-shot neural architecture search with bonas. *Advances in Neural Information Processing Systems* **33**, 1808–1819 (2020)
41. Tan, M., Chen, B., Pang, R., Vasudevan, V., Sandler, M., Howard, A., Le, Q.V.: MnasNet: Platform-aware neural architecture search for mobile. In: 2019 IEEE/CVF Conference on Computer Vision and Pattern Recognition (CVPR). pp. 2815–2823 (2019). <https://doi.org/10.1109/CVPR.2019.00293>
42. Turner, J., Crowley, E.J., O’Boyle, M., Storkey, A., Gray, G.: Blockswap: Fisher-guided block substitution for network compression on a budget (2020)
43. Veličković, P., Cucurull, G., Casanova, A., Romero, A., Liò, P., Bengio, Y.: Graph attention networks (2018)
44. Wang, C., Zhang, G., Grosse, R.: Picking winning tickets before training by preserving gradient flow (2020)
45. White, C., Neiswanger, W., Savani, Y.: Bananas: Bayesian optimization with neural architectures for neural architecture search (2020)
46. White, C., Safari, M., Sukthanker, R., Ru, B., Elsken, T., Zela, A., Dey, D., Hutter, F.: Neural architecture search: Insights from 1000 papers (2023)
47. White, C., Zela, A., Ru, B., Liu, Y., Hutter, F.: How powerful are performance predictors in neural architecture search? (2021)
48. Xiao, L., Pennington, J., Schoenholz, S.: Disentangling trainability and generalization in deep neural networks. In: International Conference on Machine Learning. pp. 10462–10472. PMLR (2020)
49. Xie, S., Zheng, H., Liu, C., Lin, L.: Snas: stochastic neural architecture search. arXiv preprint arXiv:1812.09926 (2018)
50. Xu, J., Zhao, L., Lin, J., Gao, R., Sun, X., Yang, H.: KNAS: Green neural architecture search. In: Proceedings of ICML 2021 (2021)
51. Xu, Y., Xie, L., Zhang, X., Chen, X., Qi, G.J., Tian, Q., Xiong, H.: PC-DARTS: Partial channel connections for memory-efficient architecture search. In: International Conference on Learning Representations (2020)
52. Yang, G.: Scaling limits of wide neural networks with weight sharing: Gaussian process behavior, gradient independence, and neural tangent kernel derivation (2020)
53. Ying, C., Klein, A., Real, E., Christiansen, E., Murphy, K., Hutter, F.: Nas-bench-101: Towards reproducible neural architecture search (2019)
54. Zhou, H., Yang, M., Wang, J., Pan, W.: Bayesnas: A bayesian approach for neural architecture search. In: International conference on machine learning. pp. 7603–7613. PMLR (2019)
55. Zoph, B., Vasudevan, V., Shlens, J., Le, Q.V.: Learning transferable architectures for scalable image recognition. In: Proceedings of the IEEE conference on computer vision and pattern recognition. pp. 8697–8710 (2018)

6 Appendix

This documentation includes supplemental material such as additional figures or tables, and more detailed analyses of experiments presented in the paper *TG-NAS: Leveraging Zero-Cost Proxies with Transformer and Graph Convolution Networks for Efficient Neural Architecture Search*.

6.1 Additional Ranking Figures of TG-NAS vs. Ground Truth on NAS-bench-201

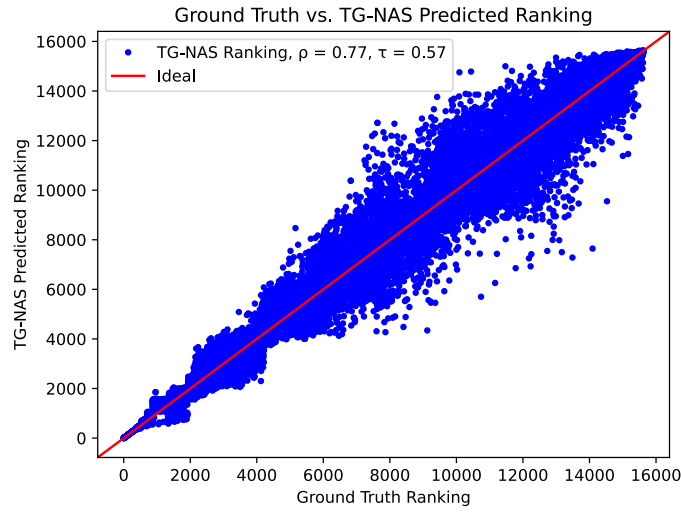


Fig. 6: TG-NAS vs. Ground Truth ranking of CIFAR-10 on NAS-bench-201

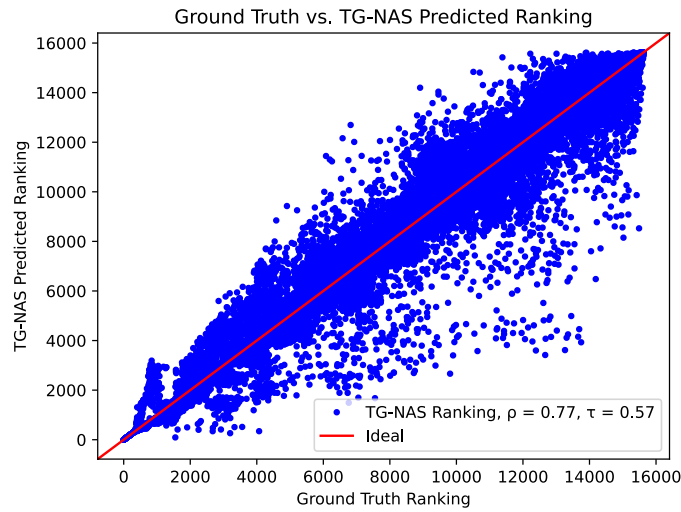


Fig. 7: TG-NAS vs. Ground Truth ranking of CIFAR-100 on NAS-bench-201

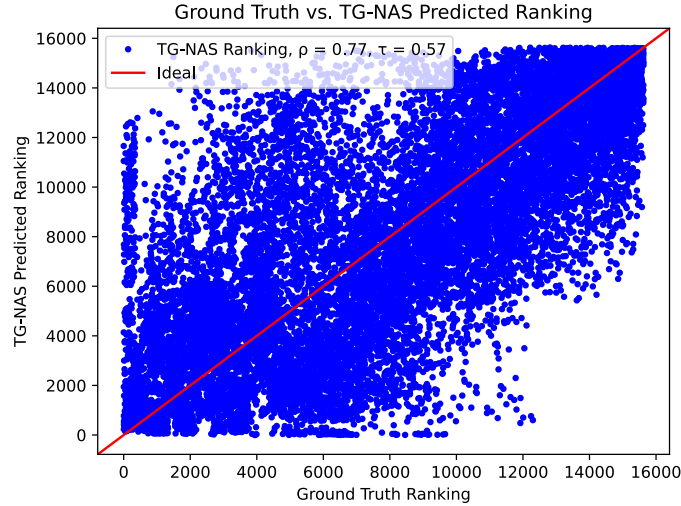


Fig. 8: TG-NAS vs. Ground Truth ranking of ImageNet16-120 on NAS-bench-201

In this section, we present additional ranking vs. ground truth figures for CIFAR-10, CIFAR-100, and ImageNet16-120 datasets on the NAS-bench-201 space. The TG proxy GCN model utilized here is trained using the entire NAS-bench-101 benchmark with CIFAR-10 accuracy results only.

We observe a positively correlated trend, with the quality of the prediction ranked as $CIFAR-10 > CIFAR-100 > ImageNet16-120$, which is expected since the training data only contain ground truth CIFAR-10 accuracy.

We believe that incorporating more diverse benchmarks, including additional evaluation results from different datasets on the same architectures, will enhance the stability and generalizability of our TG-NAS approach.

6.2 Additional Zero Cost Proxies Correlation Figures of CIFAR-100 and ImageNet16-120 Dataset on NAS-Bench-201

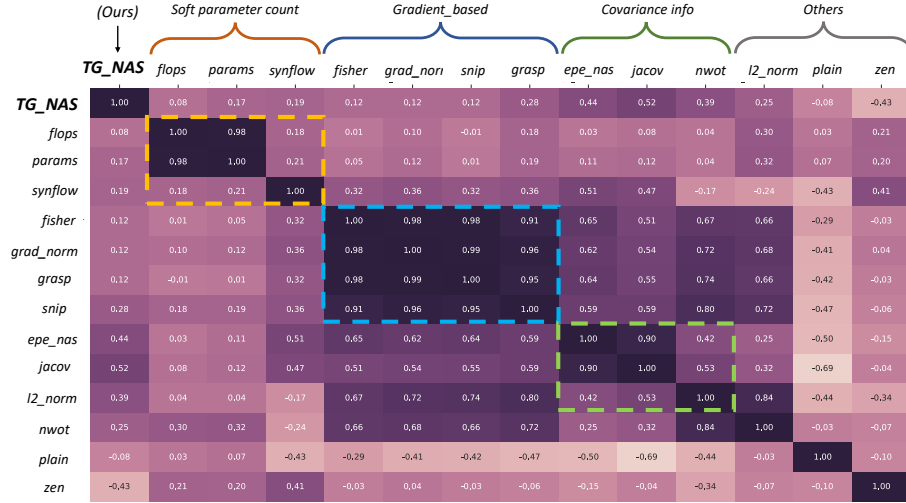


Fig. 9: Spearman’s ρ Correlation for All Pairs of ZC Proxies of CIFAR-100 on NAS-Bench-201

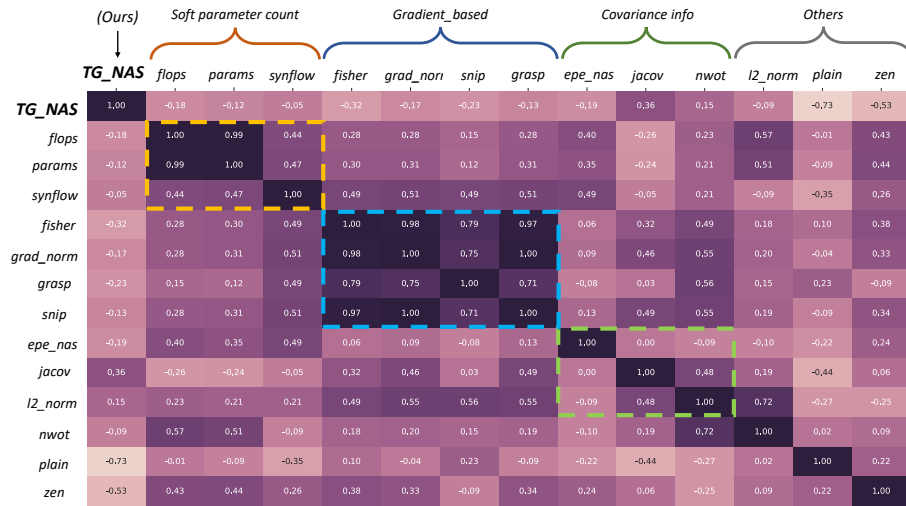


Fig. 10: Spearman’s ρ Correlation for All Pairs of ZC Proxies OF ImageNet16-120 on NAS-Bench-201